

RSDiff: Remote Sensing Image Generation from Text Using Diffusion Model

Ahmad Sebaq
Nile University
a.sebaq@nu.edu.eg

Mohamed ElHelw
Nile University
melhelw@nu.edu.eg

Abstract

Satellite imagery generation and super-resolution are pivotal tasks in remote sensing, demanding high-quality, detailed images for accurate analysis and decision-making. In this paper, we propose an innovative and lightweight approach that employs two-stage diffusion models to gradually generate high-resolution Satellite images purely based on text prompts. Our innovative pipeline comprises two interconnected diffusion models: a Low-Resolution Generation Diffusion Model (LR-GDM) that generates low-resolution images from text and a Super-Resolution Diffusion Model (SRDM) conditionally produced. The LR-GDM effectively synthesizes low-resolution by (computing the correlations of the text embedding and the image embedding in a shared latent space), capturing the essential content and layout of the desired scenes. Subsequently, the SRDM takes the generated low-resolution image and its corresponding text prompts and efficiently produces the high-resolution counterparts, infusing fine-grained spatial details and enhancing visual fidelity. Experiments are conducted on the commonly used dataset, Remote Sensing Image Captioning Dataset (RSICD). Our results demonstrate that our approach outperforms existing state-of-the-art (SoTA) models in generating satellite images with realistic geographical features, weather conditions, and land structures while achieving remarkable super-resolution results for increased spatial precision.

1. Introduction

Satellite imagery is crucial in various domains, including remote sensing, climate monitoring, and urban planning [6]. The ability to generate high-quality satellite images from text prompts has significant implications for data augmentation, simulation, and enhancing the accessibility of satellite data in resource-constrained environments [35, 38]. Traditional methods for generating satellite images often rely on convolutional neural networks (CNNs) [27] or generative adversarial networks (GANs) [7], but they demand large datasets and considerable computational resources [1, 3, 39].

Diffusion models [9] offer several benefits in the realm of data generation. Firstly, they provide a powerful framework for modeling complex distributions in high-dimensional spaces. By iteratively applying a diffusion process, these models can capture intricate dependencies and generate realistic samples that align with the true underlying data distribution. This capability makes diffusion models well-suited for tasks such as data augmentation, where diverse and plausible samples are required to enhance the training process of deep learning models.

In the domain of image super-resolution, diffusion models also bring noteworthy advantages [10]. One key strength lies in their ability to generate high-quality images at different resolutions through a sequential process. By starting with a lower-resolution image and gradually refining it, diffusion models excel at capturing global dependencies and preserving fine details. This step-wise approach allows for efficient processing and facilitates the modeling of realistic textures and structures in real-world images. Moreover, diffusion models can be trained using large-scale datasets, enabling the acquisition of prior knowledge that aids in producing visually appealing and faithful super-resolved images.

In this paper, we present a pioneering approach that leverages the power of diffusion models to generate satellite images from text prompts. We propose a novel pipeline composed of two diffusion models: an LR-GDM and a SRDM. The LR-GDM generates low-resolution satellite images from text prompts, capturing the essential content and layout of the desired scenes. The SRDM then takes these low-resolution images as input and super-resolves them, infusing fine-grained spatial details and enhancing visual fidelity to produce high-resolution satellite images. This dual diffusion model approach enables us to generate realistic and visually compelling satellite imagery aligned with the specified textual descriptions.

The main contributions of this work are as follows:

- We propose a novel pipeline that combines two diffusion models, allowing us to generate high-resolution satellite images from text prompts efficiently. The stepwise generation process ensures better control over

image synthesis and enhanced spatial precision.

- Experiments show that our diffusion pipeline performs better on satellite image synthesis. It achieves the new Fréchet Inception Distance (FID) SoTA for image synthesis with only ~ 0.75 billion parameters in total.

2. Related Work

2.1. Generative Adversarial Networks

The challenge of generating images from textual descriptions is a significant and complex undertaking, with the objective of producing realistic visuals based on natural language prompts. The initial investigations into text-to-image generation predominantly center around algorithms based on GANs. The initial groundbreaking research involves the utilization of a text-conditional GAN [3]. In this framework, the generator is specifically engineered to produce realistic images by leveraging extracted text properties and deceiving the discriminator. Conversely, the discriminator's objective is to accurately distinguish whether the input image is authentic or fabricated. Nevertheless, this particular approach is limited to producing images that possess a spatial dimension of 128x128.

In order to enhance the spatial resolution of generated images, scholars have explored the inclusion of important point locations as supplementary input for the generator. Reed et al [21]. proposed the utilization of the generative adversarial what-where network as a means to synthesize images with a spatial scale of 128x128. Another notable contribution is the StackGAN framework [37], which introduces the concept of synthesizing images using a stacked generator, as proposed by the authors. Although the initial generator produces images of limited quality, measuring just 64x64 in spatial scale, the subsequent generator will utilize these images as input and enhance their synthesis to a larger dimension of 256x256.

2.2. Diffusion Probabilistic Models

In addition to the utilization of GAN-based techniques, current studies have placed emphasis on the exploration of transformer-based models. One of the most notable works in the field is DALL-E, which can be seen as a derivative of GPT-3 (generative pre-trained transformer-3) [2] with a parameter count of 12 billion [20]. Due to the remarkable capacity for learning exhibited by the huge transformer model and the extensive training data consisting of 250 million text-image pairs, DALL-E demonstrates the capability to effectively merge disparate linguistic concepts and generate visually impressive images with a spatial resolution of 256 x 256. The publication of the second iteration of DALL-E has occurred in the recent past [19]. DALL-E 2 exhibits enhanced capabilities in comparison to its predecessor, DALL-E 1, since it employs a more

sophisticated artificial intelligence framework. Similar to the CLIP (contrastive language–image pre-training) model [16], DALL-E 2 acquires knowledge by directly assimilating the association between images and textual descriptions. The diffusion model is capable of producing high-quality images, both realistic and artistic in nature, with a spatial resolution of 1024x1024. These images are generated by leveraging the provided text descriptions.

Currently, the majority of research efforts have been directed toward the development of natural images. However, the corresponding studies within the remote sensing community remain underdeveloped. The generation of realistic remote sensing images from text descriptions continues to be a problem due to the increased demands for authenticity and plausibility in application scenarios of remote sensing jobs.

3. Methodology

The predominant focus of current research in the remote sensing domain pertaining to text-to-image generation lies in the realm of GAN-based methodologies [1, 3, 39]. In contrast, the proposed method centers around a diffusion-based technique. The primary component of our approach is the sequential progression of numerous diffusion processes. The pipeline consists of two diffusion models. Given the considerable success and exceptional output quality of Imagen [24], we opted to adopt a similar technique in our pipeline. The architecture of our model comprises a text encoder responsible for transforming text into a series of embeddings. Additionally, it incorporates a series of conditional diffusion models that progressively convert these embeddings into images with higher resolutions.

3.1. Pretrained text encoders

Language models [4, 18] are trained on a corpus consisting solely of text, which is notably bigger in size compared to paired image-text data. As a result, these models are exposed to a vast and diverse distribution of textual information. The size of these models is typically larger than the text encoders seen in existing image-text models. Therefore, it is logical to investigate both categories of text encoders for the task of text-to-image conversion. Pretrained text encoder T5 [17, 18] is utilized in our approach as it uses a unified framework where all tasks, both generation, and classification, are treated as text-to-text problems. Also, T5 is hybrid as it is trained to output one word or multiple words for one mask. This allows the model to be flexible in learning the language structure. To ensure simplicity, the weights of the text encoder are held constant. The process of freezing offers numerous benefits, including the ability to do offline computation of embeddings. This feature leads to minimal computational requirements and memory use for

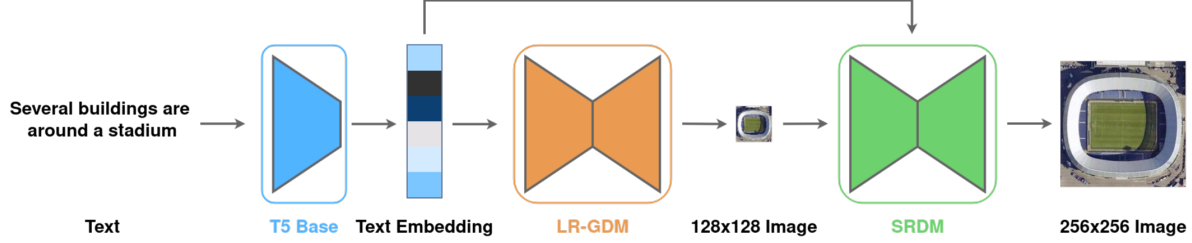


Figure 1. The RSDiff framework utilizes the T5 text encoder for the purpose of encoding the input text into text embeddings. The conditional diffusion model is utilized to transform the text embedding into a 128x128 picture. RSDiff employs text-conditioned super-resolution diffusion models to do image upsampling, increasing the image resolution to 256x256 pixels.

training the text-to-image model. As mentioned in [24], it is evident that increasing the size of the text encoder enhances the quality of text-to-image generation.

3.2. Diffusion models and classifier-free guidance

Diffusion models [9, 29, 30] belong to a category of generative models that transform Gaussian noise into samples derived from a learned data distribution using an iterative denoising procedure. The models have the capability to be conditional, such as being dependent on class labels, text, or low-resolution photos [5, 10, 14, 19, 23, 25, 33].

The training of a diffusion model $\hat{\mathbf{x}}_\theta$ involves the utilization of a denoising objective, which has the following form:

$$\mathbb{E}_{\mathbf{x}, \mathbf{c}, \epsilon, t} [w_t \|\hat{\mathbf{x}}_\theta(\alpha_t \mathbf{x} + \sigma_t \epsilon, \mathbf{c}) - \mathbf{x}\|_2^2] \quad (1)$$

Where (\mathbf{x}, \mathbf{c}) represent pairs of data and their corresponding conditioning factors, $t \sim \mathcal{U}([0, 1])$, $\epsilon \sim \mathcal{N}(\mathbf{0}, \mathbf{I})$, and α_t, σ_t, w_t are functions that impact the quality of the sample. $\hat{\mathbf{x}}_\theta$ is trained in a manner that aims to remove noise from $\mathbf{z}_t := \alpha_t \mathbf{x} + \sigma_t \epsilon$ and produce \mathbf{x} , utilizing a squared error loss function that is weighted to prioritize specific values of t .

The utilization of classifier guidance [5] is a method employed to enhance the quality of samples and decrease variability in conditional diffusion models. This is achieved by including gradients derived from a pre-trained model, namely $p(c|z_t)$, during the sampling process. The utilization of classifier-free guidance [11] approach presents an alternate methodology that circumvents the reliance on a pre-trained model. Instead, it involves the simultaneous training of a solitary diffusion model on both conditional and unconditional objectives. This is achieved by randomly deleting a specific parameter, denoted as c during the training process, typically with a chance of 10%. The process of sampling is carried out with the adjusted \mathbf{x} -prediction technique:

$$\hat{\epsilon}_\theta(\mathbf{z}_t, \mathbf{c}) = w \epsilon_\theta(\mathbf{z}_t, \mathbf{c}) + (1 - w) \epsilon_\theta(\mathbf{z}_t) \quad (2)$$

Here, $\epsilon_\theta(\mathbf{z}_t, \mathbf{c})$ and $\epsilon_\theta(\mathbf{z}_t)$ are conditional and unconditional ϵ -predictions, given by $\epsilon_\theta := (\mathbf{z}_t - \alpha_t \hat{\mathbf{x}}_\theta) / \sigma_t$ and w is

the guidance weight. When the value of w is set to 1, the classifier-free guidance is disabled, but increasing the value of w above 1 enhances the impact of guidance. The effectiveness of text conditioning in RSDiff relies heavily on the utilization of classifier-free advice.

3.3. Cascaded diffusion models

The proposed methodology involves employing a sequential process consisting of a foundational 128x128 model, alongside text-conditioned super-resolution diffusion models, to enhance the resolution of a generated image from 128 x 128 to 256 x 256. The utilization of cascaded diffusion models, together with noise conditioning augmentation, has proven to be highly successful in the gradual generation of images with a high level of fidelity [10]. In addition, incorporating noise level conditioning into the super-resolution models enhances the quality of the generated samples and increases the resilience of these models in handling artifacts produced by lower-resolution models [10]. Noise conditioning augmentation is employed for both of the super-resolution models. This aspect is deemed crucial in the production of photographs with a high level of accuracy and detail. The low-resolution image is subjected to corruption by augmentation, based on a given conditioning level. Subsequently, the diffusion model is conditioned on the augmented image. During the training phase, the amount of augmentation is selected in a random manner. However, during the inference phase, we systematically explore various values of augmentation in order to identify the optimal sample quality. In this study, Gaussian noise is employed as a means of augmentation, and we implement variance-preserving Gaussian noise augmentation that mimics the forward process utilized in diffusion models.

3.4. Neural network architecture

The U-Net architecture [15] is modified for the base 128x128 text-to-image diffusion model. The network incorporates text embeddings by utilizing a pooled embedding vector, which is combined with the diffusion timestep

embedding in a manner similar to the class embedding conditioning technique [5, 10]. In order to enhance our model and also keep it light, we used only 4 upsampling and down-sampling stages, we incorporated cross-attention across the text embeddings at the last 3 stages by conditioning on the complete sequence of text embeddings. In addition, we also used Layer Normalisation in the attention and pooling layers of text embeddings which significantly enhanced performance. We used only 3 residual blocks for upsampling and downsampling the activations [31].

The Efficient U-Net model [24], is employed for achieving super-resolution from 128x128 to 256x256. We harvested its improvements to enhance memory efficiency, reduce inference time, and improve convergence speed, but we used the self-attention layer only in the last stage of the upsampling and downsampling. We also kept the last text cross-attention layers which we found to be critical.

We decided to generate a 128x128 image and then super-resolve it to 256x256 instead of generating a 256x256 image in one step, several factors influenced this approach:

- **Computational efficiency:** Diffusion models can be computationally intensive, especially when applied to high-resolution images. By initially generating a lower-resolution image, we can alleviate the computational burden, resulting in faster processing and training times. This approach enables more practical implementation and facilitates experimentation with larger datasets.
- **Enhanced information flow:** Diffusion models often operate in an autoregressive manner, processing a sequence of lower-resolution images or noise samples. Starting with a lower resolution allows for better information flow and conditioning at each step of the diffusion process. This sequential generation aids in accurately modeling the data distribution and capturing complex dependencies within the image.
- **Capturing global dependencies:** Generating a lower-resolution image initially enables diffusion models to capture global dependencies and structures more effectively. This step allows the model to learn the overarching patterns and relationships present in the image. By utilizing this understanding, the subsequent super-resolution process can ensure that the resulting high-resolution image aligns with the overall structure of the target image.
- **Prioritization of details:** The initial lower-resolution generation in diffusion models allows for the prioritization of important image details and textures during the subsequent super-resolution step. By focusing on recovering these critical aspects, the model can produce enhanced high-resolution images that

preserve realistic and fine-grained details. This is particularly advantageous in real-world image super-resolution tasks, where capturing and preserving such details are essential for generating visually pleasing and faithful results.

4. Experiments

4.1. Dataset

The Remote Sensing Image Captioning Dataset (RSICD) [13] was utilized to assess the proposed methodology in this investigation. The RSICD dataset was initially gathered specifically for the purpose of facilitating the remote sensing picture captioning assignment. The dataset comprises a comprehensive collection of 10,921 remote-sensing photos with excellent resolution. Every image in the dataset possesses dimensions of 224x224 pixels and is accompanied by five textual descriptions as annotations. The dataset consists of 30 distinct scene classes, namely airport, bare land, baseball field, beach, bridge, center, church, commercial, dense residential, desert, farmland, forest, industrial, meadow, medium residential, mountain, parking, park, playground, pond, port, railway station, resort, river, school, sparse residential, square, stadium, storage tanks, and viaduct. For the experiment, the training set consists of 8734 text-image pairings from the training split, while the test set comprises the remaining 2187 text-image pairs [36]. In the experiment, all photos were resized to a resolution of 256x256.

4.2. Evaluation metrics

The evaluation metrics employed in this study are the Inception Score (IS) [26] and the FID [8]. These metrics are utilized to assess the degree of stylistic resemblance between the generated images and the original samples [16, 40] in the RSICD. In this context, the function $g(z)$ represents the image that is formed and needs to be assessed. Additionally, $q(l|x)$ refers to the posterior probability of a specific label, denoted as l , which is computed by the Inception-V3 model for a given image x . Then, IS can be calculated as:

$$IS = \exp[\mathbb{E}_{z \sim q(z)}[D_{kl}(q(l|g(z))||q(l))]] \quad (3)$$

The marginal class distribution is $q(l)$ and $D_{kl}(\cdot)$ refers to the KL-divergence, which is a measure of the difference between two probability distributions.

The FID score is computed using the features derived from the final average pooling layer in the Inception-V3 model. Then, IS can be calculated as:

$$FID = \|\mu_r - \mu_g\|^2 + Tr((\Sigma_r + \Sigma_g - 2(\Sigma_r \Sigma_g)^{\frac{1}{2}}) \quad (4)$$

Where (μ_r, Σ_r) and (μ_g, Σ_g) represent the mean and covariance of the real and generated features, respectively.

The function $Tr(\cdot)$ denotes the trace operation in linear algebra.

4.3. Training

A significantly lighter diffusion model is employed for image synthesis consisting of 260 million parameters compared to the one utilized in Imagen [24] which consists of 2 billion parameters. Additionally, a 260 million parameter model is employed for super-resolution tasks which is also lighter than the one used in Imagen with 600 million parameters. Both models were trained using a batch size of 64 and 1000 training epochs. The base 128x128 model in our study utilizes the Tesla V100 SXM2 processor, which is equipped with 32GB of memory. Additionally, the super-resolution variant employs another Tesla V100 chip. The Adafactor optimizer [28] is employed for our standard 128x128 model due to its significantly reduced memory requirements compared to Adam while attaining comparable performance. The Adam optimizer [12] is preferred over Adafactor for super-resolution models due to its superior performance. We used a learning rate of $1e-4$ with 10,000 linear warmup steps for both optimizers. To provide classifier-free guidance, we engage in joint training by randomly setting the text embeddings to zero with a probability of 10% for all three models.

5. Results

We assess the qualitative performance of the suggested method in comparison to 7 current SoTA approaches. A concise overview of various strategies is provided below.

- **Attn-GAN:** Fine-grained text-to-image generation based on GAN with attention learning and multi-stage refinement [34].
- **DAE-GAN:** Aspect-level text-to-image synthesis with attended global refinement and aspect-aware local refinement [22].
- **DF-GAN:** GAN-based text-to-image generation using the deep text-image fusion block and a target-aware discriminator [32].
- **Lafite:** Language-free text-to-image generation with the pre-trained CLIP model [40].
- **DALL-E:** Zero-shot text-to-image generation using the modified GPT-3 model [19].
- **Txt2Img-MHN (VQVAE):** Text-to-image modern Hopfield network with image encoder and decoder from VQVAE [36].
- **Txt2Img-MHN (VQGAN):** Text-to-image modern Hopfield network with image encoder and decoder from VQGAN [36].

- **RSDiff (Ours):** The proposed text-to-image cascaded diffusion models pipeline.

The generation of remote sensing images that are both photo-realistic and semantic-consistent is a highly demanding task, mostly because of the intricate spatial distribution of many ground objects. Although DF-GAN and other advanced GAN-based techniques have demonstrated impressive capabilities in replicating the visual style of remote sensing images, they may encounter challenges when it comes to accurately reproduce intricate shape and boundary details of complex ground targets, such as the playground (located in the 7th row of Table 2) and the stadium (located in the 9th row of Table 2). In contrast, the suggested RSDiff algorithm has the capability to produce more realistic outcomes in these complex settings.

Furthermore, it has been observed that RSDiff exhibits superior ability in acquiring the notion of amount. Consider the last three rows depicted in Table 2 as an illustrative example. The three input text descriptions provided by the user pertain to the subject of building objects. However, the number of buildings mentioned in these descriptions varies, ranging from a singular building to many buildings, and finally to a large number of buildings. While the majority of the solutions yield satisfactory outcomes in the initial scenario, comprehending the precise meaning of terms such as "several" and "many" poses a greater challenge. This tendency is most evident in the outcome of Lafite when it erroneously produces a substantial number of densely populated residential structures when presented with textual descriptions of "several buildings." In contrast, the outcomes of RSDiff exhibit a higher degree of semantic consistency with the textual descriptions provided as input.

Assessing the quality of synthesized images typically relies on human observers' visual perception, which is often intuitive. However, accurately quantifying this judgment poses challenges due to the inherent ambiguity and complexity of the semantic information conveyed within the image. Presently, the prevailing metrics employed for image generation encompass the Inception Score and the FID Score [14, 20]. Although these two measures are straightforward in nature, they were initially employed to assess the efficacy of the GAN model, with an emphasis on either the resemblance of visual styles or the disparity in features between synthesized and authentic data.

Table 1 presents a comprehensive overview of the Inception Score and FID Score associated with each approach employed in the present investigation. One intriguing observation is that GAN-based techniques tend to exhibit significantly superior performance on metrics such as the Inception Score and FID Score compared to Transformer-based methods, a finding that aligns with earlier research [20]. The Attn-GAN, outperforms the proposed RSDiff model, producing an Inception Score of 11.71 compared to RSD-

Test prompt	Attn-GAN	DAE-GAN	DF-GAN	Lafite	DALL-E	Txt2Img-MHN (VQVAE)	Txt2Img-MHN (VQGAN)	RSDiff (Ours)	Real Image
An airport with many buildings beside in it									
There is no plant on the bare land									
A baseball field is near some green trees									
In front of the sea is a vast beach									
There is a long bridge over the river									
Narrow roads were built around the farm									
Next to the playground is a house with a grey roof									
A large number of white ships were parked around the harbor									
Several buildings are around a stadium									
Many buildings are in two sides of a railway station									
Many green trees are around a building with a swimming pool									
On the ground there are several residential buildings									
Many buildings and green trees are in a dense residential area									

Table 1. Demonstration of remote sensing images produced utilizing diverse text-to-image generation techniques, all derived from the textual descriptions within the test dataset.

iff's 7.22. Simultaneously, it's important to recognize that RSDiff, despite its slightly lower score, holds a notable position as a leading diffusion model. Moreover, pivoting to a different evaluation metric, the suggested methodology shines with remarkable performance in FID score, attaining a state-of-the-art outcome of 66.49.

6. Conclusion

This paper introduces a novel text-to-image diffusion model that aims to generate remote-sensing images that are both photo-realistic and semantically compatible with the given text descriptions. Furthermore, we conduct a thor-

Method	Inception Score \uparrow	FID Score \downarrow
Attn-GAN	11.71	95.81
DAE-GAN	7.71	93.15
DF-GAN	9.51	109.41
Lafite	10.70	74.11
DALL-E	2.59	191.93
RSDiff (Ours)	7.22	66.49
Txt2Img-MHN (VQVAE)	3.51	175.36
Txt2Img-MHN (VQGAN)	5.99	102.44

Table 2. The quantitative results obtained on the RSICD test set. The inception score and the FID score are reported in our study.

ough comparison and analysis of the performance of our model in relation to previous methodologies.

The results obtained from a series of comprehensive tests conducted on the RSICD benchmark remote sensing text-image dataset provide evidence that the proposed method has the capability to generate remote sensing images that exhibit a higher degree of realism compared to existing methodologies.

A primary obstacle encountered in the process of generating remote-sensing images from textual descriptions is the scarcity of text-image pairs available in the training dataset. Acquiring precise textual descriptions for remote sensing data is typically challenging, although a substantial volume of unlabeled high-resolution remote sensing photos is readily available. Therefore, further investigation is warranted to explore the potential of leveraging the copious semantic data present in unlabeled photos for enhancing the efficacy of text-to-image generation. In our forthcoming research endeavors, we shall endeavor to delve into the intricacies of this subject matter.

References

- [1] Mesay Belete Bejiga, Farid Melgani, and Antonio Vascotto. Retro-remote sensing: Generating images from ancient texts. *IEEE Journal of Selected Topics in Applied Earth Observations and Remote Sensing*, 12(3):950–960, 2019. [1](#), [2](#)
- [2] Tom Brown, Benjamin Mann, Nick Ryder, Melanie Subbiah, Jared D Kaplan, Prafulla Dhariwal, Arvind Neelakantan, Pranav Shyam, Girish Sastry, Amanda Askell, et al. Language models are few-shot learners. *Advances in neural information processing systems*, 33:1877–1901, 2020. [2](#)
- [3] Chen Chen, Hongxiang Ma, Guorun Yao, Ning Lv, Hua Yang, Cong Li, and Shaohua Wan. Remote sensing image augmentation based on text description for waterside change detection. *Remote Sensing*, 13(10):1894, 2021. [1](#), [2](#)
- [4] Jacob Devlin, Ming-Wei Chang, Kenton Lee, and Kristina Toutanova. Bert: Pre-training of deep bidirectional transformers for language understanding. *arXiv preprint arXiv:1810.04805*, 2018. [2](#)
- [5] Prafulla Dhariwal and Alexander Nichol. Diffusion models beat gans on image synthesis. *Advances in neural information processing systems*, 34:8780–8794, 2021. [3](#), [4](#)
- [6] Pedram Ghamisi, Javier Plaza, Yushi Chen, Jun Li, and Antonio J Plaza. Advanced spectral classifiers for hyperspectral images: A review. *IEEE Geoscience and Remote Sensing Magazine*, 5(1):8–32, 2017. [1](#)
- [7] Ian Goodfellow, Jean Pouget-Abadie, Mehdi Mirza, Bing Xu, David Warde-Farley, Sherjil Ozair, Aaron Courville, and Yoshua Bengio. Generative adversarial nets. *Advances in neural information processing systems*, 27, 2014. [1](#)
- [8] Martin Heusel, Hubert Ramsauer, Thomas Unterthiner, Bernhard Nessler, and Sepp Hochreiter. Gans trained by a two time-scale update rule converge to a local nash equilibrium. *Advances in neural information processing systems*, 30, 2017. [4](#)
- [9] Jonathan Ho, Ajay Jain, and Pieter Abbeel. Denoising diffusion probabilistic models. *Advances in neural information processing systems*, 33:6840–6851, 2020. [1](#), [3](#)
- [10] Jonathan Ho, Chitwan Saharia, William Chan, David J Fleet, Mohammad Norouzi, and Tim Salimans. Cascaded diffusion models for high fidelity image generation. *The Journal of Machine Learning Research*, 23(1):2249–2281, 2022. [1](#), [3](#), [4](#)
- [11] Jonathan Ho and Tim Salimans. Classifier-free diffusion guidance. *arXiv preprint arXiv:2207.12598*, 2022. [3](#)
- [12] Diederik P Kingma and Jimmy Ba. Adam: A method for stochastic optimization. *arXiv preprint arXiv:1412.6980*, 2014. [5](#)
- [13] Xiaoqiang Lu, Binqiang Wang, Xiangtao Zheng, and Xuelong Li. Exploring models and data for remote sensing image caption generation. *IEEE Transactions on Geoscience and Remote Sensing*, 56(4):2183–2195, 2017. [4](#)
- [14] Alex Nichol, Prafulla Dhariwal, Aditya Ramesh, Pranav Shyam, Pamela Mishkin, Bob McGrew, Ilya Sutskever, and Mark Chen. Glide: Towards photorealistic image generation and editing with text-guided diffusion models. *arXiv preprint arXiv:2112.10741*, 2021. [3](#), [5](#)
- [15] Alexander Quinn Nichol and Prafulla Dhariwal. Improved denoising diffusion probabilistic models. In *International Conference on Machine Learning*, pages 8162–8171. PMLR, 2021. [3](#)

[16] Alec Radford, Jong Wook Kim, Chris Hallacy, Aditya Ramesh, Gabriel Goh, Sandhini Agarwal, Girish Sastry, Amanda Askell, Pamela Mishkin, Jack Clark, et al. Learning transferable visual models from natural language supervision. In *International conference on machine learning*, pages 8748–8763. PMLR, 2021. [2](#), [4](#)

[17] Colin Raffel, Minh-Thang Luong, Peter J Liu, Ron J Weiss, and Douglas Eck. Online and linear-time attention by enforcing monotonic alignments. In *International conference on machine learning*, pages 2837–2846. PMLR, 2017. [2](#)

[18] Colin Raffel, Noam Shazeer, Adam Roberts, Katherine Lee, Sharan Narang, Michael Matena, Yanqi Zhou, Wei Li, and Peter J Liu. Exploring the limits of transfer learning with a unified text-to-text transformer. *The Journal of Machine Learning Research*, 21(1):5485–5551, 2020. [2](#)

[19] Aditya Ramesh, Prafulla Dhariwal, Alex Nichol, Casey Chu, and Mark Chen. Hierarchical text-conditional image generation with clip latents. *arXiv preprint arXiv:2204.06125*, 1(2):3, 2022. [2](#), [3](#), [5](#)

[20] Aditya Ramesh, Mikhail Pavlov, Gabriel Goh, Scott Gray, Chelsea Voss, Alec Radford, Mark Chen, and Ilya Sutskever. Zero-shot text-to-image generation. In *International Conference on Machine Learning*, pages 8821–8831. PMLR, 2021. [2](#), [5](#)

[21] Scott E Reed, Zeynep Akata, Santosh Mohan, Samuel Tenka, Bernt Schiele, and Honglak Lee. Learning what and where to draw. *Advances in neural information processing systems*, 29, 2016. [2](#)

[22] Shulan Ruan, Yong Zhang, Kun Zhang, Yanbo Fan, Fan Tang, Qi Liu, and Enhong Chen. Dae-gan: Dynamic aspect-aware gan for text-to-image synthesis supplementary document. [5](#)

[23] Chitwan Saharia, William Chan, Huiwen Chang, Chris Lee, Jonathan Ho, Tim Salimans, David Fleet, and Mohammad Norouzi. Palette: Image-to-image diffusion models. In *ACM SIGGRAPH 2022 Conference Proceedings*, pages 1–10, 2022. [3](#)

[24] Chitwan Saharia, William Chan, Saurabh Saxena, Lala Li, Jay Whang, Emily L Denton, Kamyar Ghasemipour, Raphael Gontijo Lopes, Burcu Karagol Ayan, Tim Salimans, et al. Photorealistic text-to-image diffusion models with deep language understanding. *Advances in Neural Information Processing Systems*, 35:36479–36494, 2022. [2](#), [3](#), [4](#), [5](#)

[25] Chitwan Saharia, Jonathan Ho, William Chan, Tim Salimans, David J Fleet, and Mohammad Norouzi. Image super-resolution via iterative refinement. *IEEE Transactions on Pattern Analysis and Machine Intelligence*, 45(4):4713–4726, 2022. [3](#)

[26] Tim Salimans, Ian Goodfellow, Wojciech Zaremba, Vicki Cheung, Alec Radford, and Xi Chen. Improved techniques for training gans. *Advances in neural information processing systems*, 29, 2016. [4](#)

[27] Pierre Sermanet, Soumith Chintala, and Yann LeCun. Convolutional neural networks applied to house numbers digit classification. In *Proceedings of the 21st international conference on pattern recognition (ICPR2012)*, pages 3288–3291. IEEE, 2012. [1](#)

[28] Noam Shazeer and Mitchell Stern. Adafactor: Adaptive learning rates with sublinear memory cost. In *International Conference on Machine Learning*, pages 4596–4604. PMLR, 2018. [5](#)

[29] Jascha Sohl-Dickstein, Eric Weiss, Niru Maheswaranathan, and Surya Ganguli. Deep unsupervised learning using nonequilibrium thermodynamics. In *International conference on machine learning*, pages 2256–2265. PMLR, 2015. [3](#)

[30] Yang Song and Stefano Ermon. Generative modeling by estimating gradients of the data distribution. *Advances in neural information processing systems*, 32, 2019. [3](#)

[31] Yang Song, Jascha Sohl-Dickstein, Diederik P Kingma, Abhishek Kumar, Stefano Ermon, and Ben Poole. Score-based generative modeling through stochastic differential equations. *arXiv preprint arXiv:2011.13456*, 2020. [4](#)

[32] Ming Tao, Hao Tang, Fei Wu, Xiao-Yuan Jing, Bing-Kun Bao, and Changsheng Xu. Df-gan: A simple and effective baseline for text-to-image synthesis. In *Proceedings of the IEEE/CVF Conference on Computer Vision and Pattern Recognition*, pages 16515–16525, 2022. [5](#)

[33] Jay Whang, Mauricio Delbracio, Hossein Talebi, Chitwan Saharia, Alexandros G Dimakis, and Peyman Milanfar. De-blurring via stochastic refinement. In *Proceedings of the IEEE/CVF Conference on Computer Vision and Pattern Recognition*, pages 16293–16303, 2022. [3](#)

[34] Tao Xu, Pengchuan Zhang, Qiuyuan Huang, Han Zhang, Zhe Gan, Xiaolei Huang, and Xiaodong He. Attngan: Fine-grained text to image generation with attentional generative adversarial networks. In *Proceedings of the IEEE conference on computer vision and pattern recognition*, pages 1316–1324, 2018. [5](#)

[35] Yonghao Xu and Pedram Ghamisi. Universal adversarial examples in remote sensing: Methodology and benchmark. *IEEE Transactions on Geoscience and Remote Sensing*, 60:1–15, 2022. [1](#)

[36] Yonghao Xu, Weikang Yu, Pedram Ghamisi, Michael Kopp, and Sepp Hochreiter. Txt2img-mhn: Remote sensing image generation from text using modern hopfield networks. *arXiv preprint arXiv:2208.04441*, 2022. [4](#), [5](#)

[37] Han Zhang, Tao Xu, Hongsheng Li, Shaoting Zhang, Xiaogang Wang, Xiaolei Huang, and Dimitris N Metaxas. Stackgan: Text to photo-realistic image synthesis with stacked generative adversarial networks. In *Proceedings of the IEEE international conference on computer vision*, pages 5907–5915, 2017. [2](#)

[38] Lefei Zhang and Liangpei Zhang. Artificial intelligence for remote sensing data analysis: A review of challenges and opportunities. *IEEE Geoscience and Remote Sensing Magazine*, 10(2):270–294, 2022. [1](#)

[39] Rui Zhao and Zhenwei Shi. Text-to-remote-sensing-image generation with structured generative adversarial networks. *IEEE Geoscience and Remote Sensing Letters*, 19:1–5, 2021. [1](#), [2](#)

[40] Y Zhou, R Zhang, C Chen, C Li, C Tensmeyer, T Yu, J Gu, J Xu, and T Sun. Lafite: Towards language-free training for text-to-image generation. arxiv 2021. *arXiv preprint arXiv:2111.13792*. [4](#), [5](#)